https://doi.org/10.5194/egusphere-2025-5676
Preprint. Discussion started: 19 February 2026

Larger variability of winter snow depth promotes the soil thermal regime instability over boreal high latitudes

Lingyun Ai[1], Kai Yang[2*], Feimin Zhang[1], Chenghai Wang[1], Tonghua Wu[3], Qi Qi[1], Haohui Li[1]

[1]Key Laboratory of Climate Resource Development and Disaster Prevention of Gansu Province, Research and Development Center of Earth System Model, College of Atmospheric Sciences, Lanzhou University, Lanzhou 730000, China.
[2]Institute of Mountain Hazards and Environment, Chinese Academy of Sciences, Chengdu, 610299, China
[3]Cryosphere Research Station on the Qinghai-Tibet Plateau, State Key Laboratory of Cryospheric Science and Frozen Soil Engineering, Northwest Institute of Eco-Environment and Resource, Chinese Academy of Sciences, Lanzhou, 730000, China

Correspondence to: K. Yang (kaiyang@imde.ac.cn)

Abstract. Permafrost degradation in Siberia is assessed as one of the global climate tipping elements. Soil thermal regime instability (STRI) describes the amplitude and frequency of soil temperature extremes at the interannual scale, and such thermal instability can propagate downward through the soil column and affect permafrost thermal conditions, making STRI a useful indicator of permafrost vulnerability. Yet, how STRI changes and the underlying mechanism remain poorly understood. Here, regarding soil temperature variability as a proxy of STRI on interannual scale, and through combining a merged soil temperature dataset with in-situ observations, it was detected that the subsurface (40 and 160 cm) STRI over Siberian continuous permafrost region is higher compared to other regions over boreal high latitudes, most pronounced in winter. Moreover, winter STRI across the Siberia continuous permafrost region has increased suddenly since early 1990s. Increase in STRI is particularly pronounced in regions where soil thermal regime was once stable, with increase rate of STRI exceeding 0.5 °C/10a in some regions. Statistical analyses and numerical experiments reveal that this increased STRI is strongly associated with the larger interannual variability of winter snow depth through its insulation effect, with snow depth accounting for more than 50% of the STRI increase in most regions, and influence of snow depth on STRI is detectable down to 3.6 m. These findings highlight that snow-soil interactions dominate winter soil thermal dynamics, particularly over the thick snow regions, with potential implications for permafrost stability, carbon dynamics, and ecosystem responses.

1 Introduction

In the high latitude and altitude cold regions where permafrost is widespread, the rate of temperature warming is more pronounced than in other regions (*Pepin et al.*, 2015; *You et al.,* 2021; *Rantanen et al.,* 2022). This warming is largely reflected in rising soil temperatures, which significantly influence soil hydrothermal processes and carbon-related dynamics in cold regions, with potential feedbacks to regional and global climate (*Davidson and Janssens,* 2006; *Romanovsky et al.,* 2010; *Hagerty et al.,* 2014; *Schuur et al.,* 2015; *Biskaborn et al.,* 2019; *Yang et al.,* 2023a). Therefore, studying the soil temperature variations—as a proxy for the soil thermal regime—is essential for a deeper understanding of permafrost degradation vulnerability and its feedback to climate systems.

https://doi.org/10.5194/egusphere-2025-5676
Preprint. Discussion started: 19 February 2026

In recent decades, soil temperature in boreal permafrost regions has risen rapidly (*Zhang et al.,* 2001; *Wundram et al.,* 2010; *Biskaborn et al.,* 2019). For instance, significant soil warming occurred in Russia at a rate of 0.30–0.31 °C per decade from 1975 to 2016 (*Chen et al.,* 2021). In addition, with the increasing frequency of climate extremes, soil temperature extremes have also intensified in cold regions through land-atmosphere interactions (*García-García et al.,* 2023; *Zhu et al.,* 2024), and may also contribute to air temperature extremes (*Wright et al.,* 2014; *Groisman et al.,* 2017). Furthermore, due to the heterogeneity in land surface, soil temperature extremes have spatial diversity (*Wang et al.,* 2024). The increased frequency and amplitude of these soil temperature extremes reflect an increase in soil thermal regime instability (STRI). STRI represents the amplitude and frequency of soil temperature extremes at the interannual scale. A high STRI value indicates larger interannual fluctuations and more pronounced cold–warm swings, whereas a low STRI value indicates relatively moderate interannual variability and a more stable soil thermal regime. Active layer thickness (ALT) responds with a pronounced thermal memory effect in response to soil temperature variations (*Wang et al.,* 2022). Extreme soil temperature fluctuations during the cold season can persist into the warm season through time-lag effects, influencing ALT and propagating to deeper soil layers via heat conduction, thereby modulating deep soil hydrothermal dynamics (*Li et al.,* 2021). Meanwhile, with increasing interannual cold–warm amplitudes, repeated vertical oscillations of the freeze–thaw interface and changes in freeze–thaw duration may alter soil structure and thermal properties, including the formation and melting of ice lenses, reorganization of pore structure, and increased soil thermal conductivity (*Style et al.,* 2011*; Rooney et al.,* 2022*; Liu et al.,* 2025). These changes further affect thermal dynamics, water migration, and energy exchange within the active layer, potentially leading to a deepening of the active layer and enhanced permafrost vulnerability (*Zhao et al.,* 2022*; Fu et al.,* 2023). Long-term trends in soil temperature, its relationship with ALT, and differences in soil thermal properties have been widely studied. Despite its critical role as a driver of these impacts, the spatiotemporal patterns and variability of STRI itself, particularly in boreal high latitudes, remain poorly quantified and understood. Therefore, further investigation into STRI is urgently needed to bridge this knowledge gap.

STRI is a metric derived from soil temperatures, ground surface temperatures are governed by the surface energy budget, and through vertical heat transfer, influence temperatures at greater soil depths. Consequently, STRI in surface and subsurface soil is directly or indirectly regulated by surface factors, such as vegetation conditions and snow cover (*Aalto et al.,* 2018; *Heijmans et al.,* 2022; *Zhong et al.,* 2025), as well as near-surface air temperature (*Paul et al.,* 2004; *Bittelli et al.,* 2015; *Amato et al.,* 2024). Vegetation affects soil thermal regime primarily through canopy shading, which reduces solar radiation absorbed by the ground and through evapotranspiration cooling (*García-García et al.,* 2023; *Blok et al.,* 2010; *Seneviratne et al.,* 2013; *Yang et al.,* 2023b). Air temperature influences the soil thermal regime indirectly by altering surface longwave radiation and sensible heat flux, thereby modulating the surface energy partitioning. Nevertheless, observations, reanalysis, and satellite data across the pan-Arctic region reveal that the difference between air and soil temperatures has become larger during the snow-covered seasons over recent decades, reflecting a weakening of air-soil thermal coupling under the condition of snow insulation (*Wang et al.,* 2016; *Chen et al.,* 2021; *Liu et al.,* 2023). Snow, lying above the soil,

https://doi.org/10.5194/egusphere-2025-5676
Preprint. Discussion started: 19 February 2026

influences soil thermal regime through its high albedo and thermal insulation effects (*Stieglitz et al.* 2003; *Zhang,* 2005; *Park et al.,* 2015). In high-latitude winter, due to the low solar radiation received by the land surface, the cooling effect of snow via its high albedo is limited (*Zhang,* 2005). Nevertheless, the low thermal conductivity of snow effectively reduces heat exchange between the soil and the atmosphere, helping to retain soil heat during autumn and winter, thereby enhancing soil thermal stability (*Stieglitz et al.* 2003; *Zhang,* 2005). This thermal insulation effect is closely linked to snow depth (*Zhang et al.,* 2018). Numerical experiments have shown that changes in snow depth significantly affect soil temperature in Siberian permafrost, accounting for over 50% of the anomalies in permafrost thermal state (*Park et al.,* 2015).

Over the past decades, snow across the boreal and Arctic regions has undergone significant changes (*Pulliainen et al.,* 2020; *Gottlieb et al.,* 2024). Distinct spatial heterogeneity of snow variation has been observed. For example, snow mass and cover have significantly decreased over North America, whereas Eurasia exhibits weaker or locally increasing trends (*Pulliainen et al.,* 2020). Consequently, the insulation effect of snow on soil thermal stability may also vary. Moreover, global climate models project an intensification of extreme snowfall in Northern America and Asia under future warming (*Quante et al.,* 2021; *Mudryk et al.,* 2020), potentially leading to the larger variability in snow depth. Therefore, exploring how the changed snow depth interannual fluctuation influences STRI is critical for understanding the multi-sphere interactions in cold regions.

This study focuses on two aspects: How has the STRI changed in boreal high latitudes? And what is the relationship between STRI and winter snow depth interannual fluctuation? To address these questions, we analyzed the characteristics of soil temperature interannual variability (as a proxy of the STRI) over the past 60 years (1963–2022) in boreal high latitudes, explored the role of changes in winter snow depth interannual variability in recent increased STRI, using station observations of snow depth and soil temperature, a merged soil temperature dataset, satellite-based snow water equivalent data, statistical analysis and model simulations.

2 Data and Methods

2.1 Datasets and quality control

In-situ daily observations of soil temperature (T_{soil}) at subsurface (40 and 160 cm depths) and snow depth (d_{snow}) were obtained from 51 stations across Russia for the period 1963–2022, compiled from the All-Russia Research Institute for Hydro-Meteorological Information–World Data Center (RIHMI-WDC) and the National Snow and Ice Data Center (NSIDC). All daily variables were converted to monthly means before analysis.

Seven reanalysis datasets (ERA5, ERA5-Land, GLDAS-Noah, FLDAS, CFSR, CFSv2, and MERRA-2; Table S1) were used to generate a merged monthly average T_{soil} dataset at 40 cm and 160 cm depths. All reanalysis datasets were interpolated to 0.5° × 0.625° (latitude × longitude) grid using linear interpolation. The merged dataset was produced following a skill-based ensemble approach that selected the optimal combination of reanalysis products to best represent

https://doi.org/10.5194/egusphere-2025-5676
Preprint. Discussion started: 19 February 2026

both the magnitude and standard deviation of T_{soil} (the details can be seen in Supplementary Note 1). The resulting merged T_{soil} dataset covers 1982–2022 and has been evaluated to show the highest Taylor skill scores and lowest biases among individual datasets (Figure S1).

Snow depth data were derived from GlobSnow 3.0 snow water equivalent divided by a snow density of 0.24 g/cm^3 (*Yue et al.,* 2022). GlobSnow 3.0 has 25 km spatial resolution, uses the EASE-GRID projection, covers 35°–85°N, and spans 1979–2018, excluding mountainous areas. The near-surface (2 m) air temperature (T_{air}) was obtained from the fifth-generation ECMWF atmospheric reanalysis (ERA5) which evolved from ERA-Interim. It had a spatial resolution of 0.25° × 0.25° from 1981 to 2018. Both GlobSnow 3.0 and ERA5 datasets were linearly interpolated to 0.5° × 0.625° grid to ensure spatial consistency with the merged T_{soil} dataset.

Prior to analysis, a series of quality control procedures were applied to the observations. All data were detrended in calculations of variability and correlations to eliminate the impact of global warming. During detrending, linear trends were computed and removed only for monthly time series with more than five valid years of data at each station; otherwise, the series was discarded. Based on the detrended data, a 9-year sliding standard deviation (SD; the detail given in Section 2.2) was then calculated for winter (December-January-February, DJF). If a 9-year window contained more than four missing values, its standard deviation was set to missing. Furthermore, stations with more than half of the computed SD values missing were deemed invalid and excluded from further analysis. After quality control, T_{soil} records at 40 cm and 160 cm depths were cross-checked to ensure consistency between layers. Only stations with valid data for both depths were retained, resulting in 22 out of 51 stations being used for subsequent analysis.

2.2 Calculation of interannual variability

Generally, soil thermal regime refers to the pattern of T_{soil} variations over time and depth (*Noetzli et al.,* 2009; *Jiang et al.,* 2016). Larger fluctuation in T_{soil} means more unstable soil thermal regime. Thus, in this study, T_{soil} variability was adopted as a proxy of the STRI on interannual scale, changes in T_{soil} variability quantify magnitude of STRI. Standard deviation (SD), which can reflect the dispersion of data (*Karl et al.,* 1995), was calculated to represent the variability on interannual scale. The calculation formula of SD is as follows:

$$SD = \sqrt{\frac{\sum\left(X_i - \overline{X}\right)^2}{n-1}} \quad (1)$$

where X_i represents the variable values at i^{th} year, and $\overline{X}$ is the average of the variable, n represents the sequence length (i.e., n years). A larger SD indicates an increase in variability in statistics. Following the scale of interannual (1-8 years) variability adopted in *Zhang et al.* (2024), a 9-year sliding SD was calculated to quantify changes in interannual variability. Specifically, the SD for n^{th} year was calculated using data from n-4$^{\mathrm{th}}$ year to n+4$^{\mathrm{th}}$ year.

https://doi.org/10.5194/egusphere-2025-5676
Preprint. Discussion started: 19 February 2026

2.3 Detection of statistical relationship between variables

Soil thermal regime in winter is not only influenced by d_{snow} but also related to near-surface T_{air} (*Amato et al.,* 2024; *Zhong et al.,* 2025). To isolate the independent relationship between STRI and d_{snow} variability, we firstly removed the influence of autumn (September-October-November, SON) and winter T_{air} variability using multiple linear regression (*Foster and Rahmstorf,* 2011; *Yang et al.,* 2023b; *Chen et al.,* 2024). A multiple linear regression model was constructed as follows:

$$y = a_1 x_1 + a_2 x_2 + \varepsilon \tag{2}$$

where x_1 and x_2 represent the T_{air} variability in autumn and winter, respectively; ε represents the residual variability primarily associated with d_{snow} and other minor factors. The residual T_{soil} variability (y') after removing the effects of T_{air} variability in autumn and winter was computed as:

$$y' = y - (a_1 x_1 + a_2 x_2) \tag{3}$$

Then, the linear correlation between y' and d_{snow} variability was computed to isolate the statistical relationship between them.

2.4 Numerical experiments

To overcome the unambiguous determination of causality in statistical analysis, numerical simulations were employed to verify the statistical relationship and explore the underlying physical mechanisms. This study conducted numerical experiments using the Community Land Model version 5 (CLM5) (*Lawrence et al.,* 2019), which was developed by the U.S. National Center for Atmospheric Research (NCAR). CLM5 is highly modular and capable of simulating multi-layer soil temperature, soil moisture, and multi-layer snow processes, explicitly accounting for freeze–thaw dynamics, making it particularly suitable for high-latitude permafrost studies (*Swenson and Lawrence,* 2012). The model was driven by CRUNCEPv7 meteorological forcing data, which provide high temporal resolution (6-hourly) long-term data including precipitation, air temperature, and wind, spanning 1901–2018, thereby supporting reliable multi-decadal numerical experiments (*Viovy,* 2018) and having been widely used in land surface modeling studies (*Brutsaert et al.,* 2020*; Pugh et al.,* 2020*; Zhang et al.,* 2022).

Two experiments were conducted: a control experiment (CTL), in which no imposed change was added, and an equilibrium sensitive experiment (SE), in which interannual variability of snowfall in autumn and winter (from September to February) was removed in CRUNCEPv7 data through replacing snowfall at each time step by its multi-year average. Here, snowfall was defined as precipitation occurring when near-surface air temperature is below 2 °C (*Jordan,* 1991). The difference between SE and CTL was used to assess the response of soil thermal regime to the reduction in winter d_{snow} variability. To reduce the uncertainties from the initial condition, CLM5 was firstly driven by CRUNCEPv7 data during 1948–2016 for two cycles; then, with the land surface conditions at the end of the second cycle being used for the initial

https://doi.org/10.5194/egusphere-2025-5676
Preprint. Discussion started: 19 February 2026

conditions in CTL and SE experiments. CTL and SE experiments were conducted during 1948–2016. Excluding the spin-up period from 1948–1992, only results from 1993–2016 were analyzed.

In both experiments, CLM5 was run under the frame of Community Earth System Model version 2.2.0, component set was I2000Clm50Sp, grid resolution was 0.9° × 1.25° (latitude × longitude). The CLM5 model employs a 15-layer soil column and the soil layers are discretized with finer resolution near the surface to accurately resolve near-surface soil temperature and freeze–thaw processes (*Lawrence et al.,* 2019). A fixed deep soil heat flux is imposed at the lower boundary to ensure stable thermal responses in the surface soil. Soil thermal and hydraulic properties nonlinearly depend on temperature and moisture, allowing realistic simulation of heat transfer under freezing and thawing conditions. Snow processes are represented using a multi-layer scheme, calculating snow depth, density, and thermal conductivity for each layer to accurately capture the thermal and physical properties of the snowpack. Soil and snow temperatures are integrated using a semi-implicit scheme to maintain numerical stability.

3 Results

3.1 Increased winter STRI over Siberian continuous permafrost region

Based on the merged monthly T_{soil} dataset, analysis of the spatiotemporal changes in STRI (T_{soil} interannual variability as a proxy) over the boreal high latitudes shows that, STRI has a distinct monthly evolution at both 40 cm and 160 cm depths (Figure 1a). STRI at 40 cm decreases from summer to autumn and reaches the minimum in October, then increases and peaks in January. Generally, STRI at 40 cm in winter is higher than the other months. By comparison, STRI at 160 cm exhibits a lag of approximately one to two months, beginning to increase in December and peaking in March. Although STRI at 160 cm is not the largest in winter, the increase during this season is the most pronounced. Thus, wintertime is selected as the focused season in this study.

The spatial distribution of wintertime T_{soil} interannual variability over the boreal high latitudes further indicates that, the Siberian continuous permafrost region exhibits the highest STRI (Figure 1b–d). Therefore, Siberian continuous permafrost region was identified as the typical domains for the subsequent analysis.

https://doi.org/10.5194/egusphere-2025-5676
Preprint. Discussion started: 19 February 2026

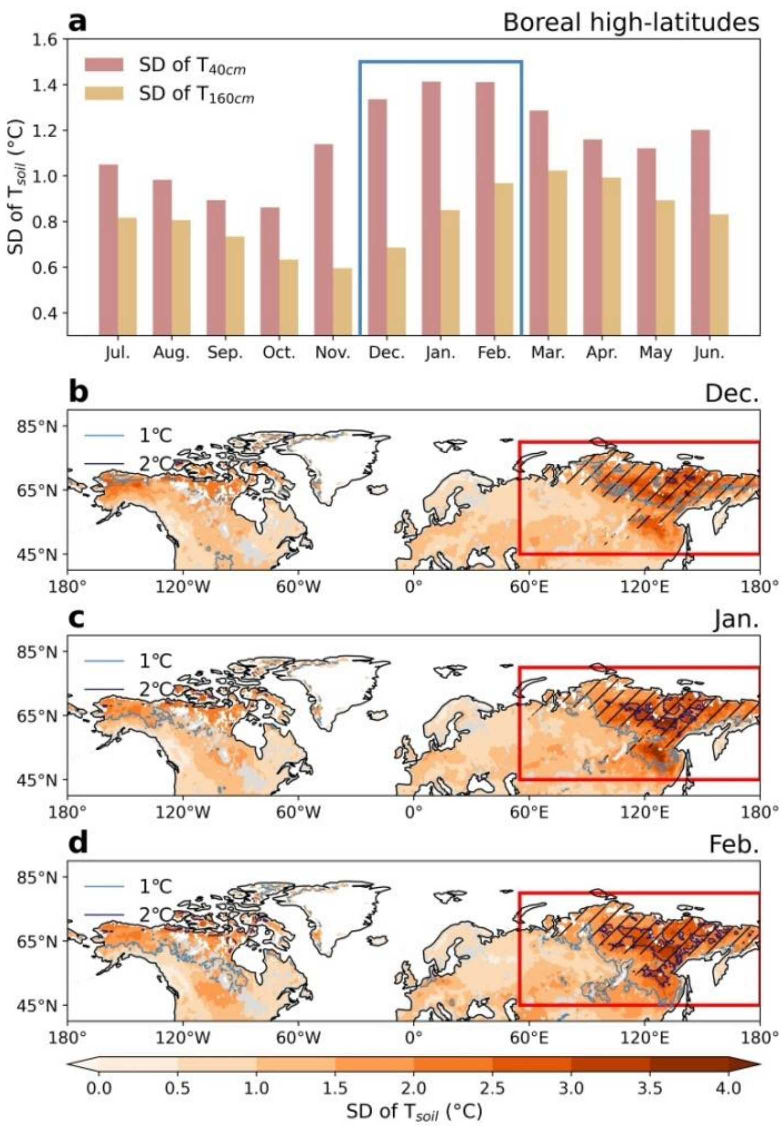

Figure 1: Spatiotemporal distribution of the STRI (T_{soil}; °C) during 1982–2022 over the boreal high-latitudes. (**a**) Monthly evolution of standard deviation (SD) of T_{soil} at 40cm and 160cm depths from September to May, which were averaged over the boreal high-latitudes. Blue rectangles indicate the winter months. (**b-d**) Spatial distribution of T_{soil} SD in winter months. Shading and contours represent SD of T_{soil} at 40 cm and 160 cm, respectively. Areas with black slant lines represent the Siberian continuous permafrost region, red rectangle mark the study domain that fully covers this region.

It has been observed that shallow-depth soil over Russia experienced significant warming during 1975–2016 (*Chen et al.*, 2021). As expected, both the merged T_{soil} dataset and in-situ observations consistently reveal that, winter T_{soil} at 40 cm and 160 cm depths show an overall warming trend over the Siberian continuous permafrost region, and significant warming still persists after the 1990s (Figure 2a). In contrast to the sustained warming, the STRI shows a long-term decreasing tendency before early 1990s, but shifts to a significant increase thereafter, which is consistently shown by the merged dataset and in-

https://doi.org/10.5194/egusphere-2025-5676
Preprint. Discussion started: 19 February 2026

situ observation (Figure 2b). This feature is further corroborated by trends derived from in-situ observations during two subperiods, which show a significant decrease in STRI over the full period (1967–2018) but a significant increase during 1993–2018 (Figure 2c). Prior to the 1990s, soil temperature increased rapidly, while interannual fluctuations were relatively weak, resulting in a low or temporarily decreasing STRI. After entering the 1990s, the rate of increase in mean soil temperature slowed, but STRI continued to rise. This may indicate that as soil temperature gradually approaches the freeze–thaw threshold, the soil thermal system becomes significantly more sensitive to external perturbations (*Paquin et al.,* 2015). Although there was a short-term increase in STRI during the 1980s, it occurred under lower background temperature conditions and had a relatively limited impact on long-term thermal stability. In contrast, the enhancement of STRI after the 1990s is more persistent and physically meaningful, possibly indicating a shift in soil thermal state from being "dominated by background warming" to being "dominated by interannual variability".

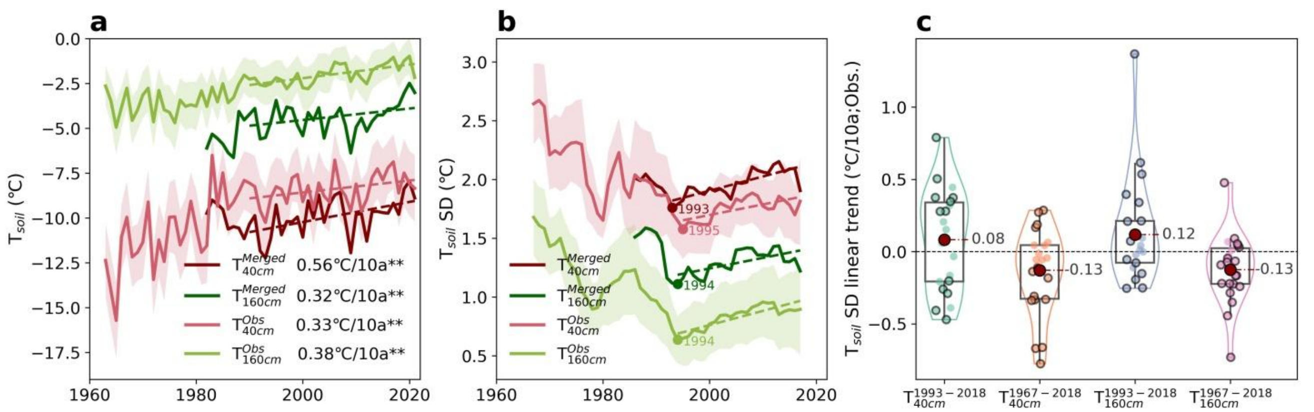

Figure 2: Temporal changes in winter STRI. **(a)** Long-term evolution of T_{soil} (°C) from the merged dataset (abbreviated as Merged; 1982–2022) and in-situ observations (abbreviated as Obs.;1963–2022) at 40 cm and 160 cm. Dashed line indicate T_{soil} trends since 1990, with '**' denoting statistically significant trends. **(b)** Evolution of winter T_{soil} interannual variability, expressed as a 9-year sliding standard deviation (SD; °C) from the merged dataset (1986–2018) and in-situ observations (1967–2018), with turning points after the 1990s labeled by years. Dashed line indicate T_{soil} SD trends since 1993, with '**' denoting statistically significant trends. **(c)** Boxplots of T_{soil} SD linear trends (°C/10a) for the full period and post-1993 based on in-situ observations, with black outlines marking statistically significant results and red dots indicating means (all significant). All significance is assessed using Student's t test with $p < 0.05$.

In addition, both the merged dataset and in-situ observations consistently indicate widespread increasing in STRI at 40 cm and 160 cm depths across Siberian continuous permafrost region since the early 1990s, with the most pronounced increases in central and western regions, where the rates of variability increase exceeding 0.5 °C/10a (Figure 3). A comparison between the 40 cm and 160 cm layers shows that although the magnitude of increase at 160 cm is smaller, the spatial pattern of the trend is largely consistent with that at 40 cm, implying that near-surface thermal perturbations might effectively propagate downward into deeper soils. Meanwhile, we note that the winter STRI exhibits negative trends in the northern part of western Siberia and eastern mountainous regions, however, the decreasing STRI trends in the northern regions are generally not statistically significant, and the eastern mountainous regions exhibit highly heterogeneous STRI patterns due to complex topography affecting snow distribution and soil thermal dynamics, thus these areas are not emphasized in this study.

https://doi.org/10.5194/egusphere-2025-5676
Preprint. Discussion started: 19 February 2026

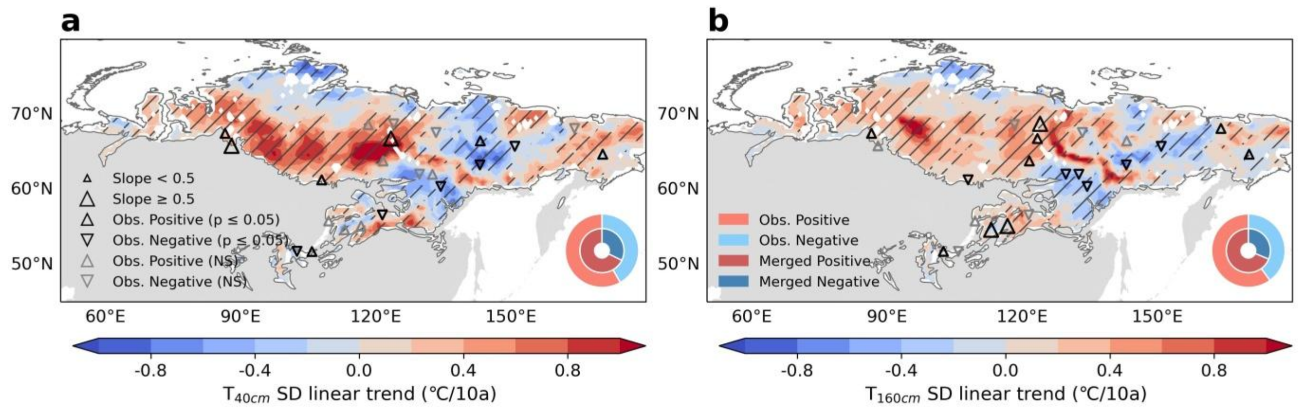

Figure 3: Spatial pattern of trends in STRI during 1993–2018. Distributions of the linear trends in T_{soil} standard deviation (SD; °C/10a) at 40 cm **(a)** and 160 cm **(b)**, based on the merged dataset (shading) and in-situ observations (triangles), shading with black hatching and triangles with black outlines denote significance. Pie charts in the lower right summarize the proportion of significant increases and decreases in T_{soil} SD from both datasets. All significance is assessed using Student's t test with $p < 0.05$.

Overall, above results demonstrate that winter STRI has increased markedly over Siberian continuous permafrost region since early 1990s, suggesting an unusual shift in the soil thermal regime.

3.2 Close linkage between increased STRI instability and greater interannual snow depth fluctuations

Soil temperature over boreal high-latitudes is influenced by multiple energy budget processes, including soil-air heat exchange which is related to factors such as air temperature, snow, or land cover (*Soong et al.*, 2020), soil heat transfer which is linked to soil properties, soil water phase change (*Yang et al.*, 2018; *Zhu et al.*, 2019), as well as the lagged effect of the antecedent soil thermal anomalies. While soil freezing over Siberia mainly occurs before winter, and thermal contrast between soil and air may be reduced substantially by the insulating effects of snow in winter. Thus, this study mainly explored the linkage between STRI and snow, effects of the other factors were also discussed.

Snow directly overlies the soil surface, influencing heat and water exchanges between soil and air. Previous studies have suggested that the snow depth (d_{snow}) and snow cover fraction can influence T_{soil} through thermal insulation effects and albedo effects (*Stieglitz et al.,* 2003; *Zhang,* 2005; *Aalto et al.,* 2018). In the Siberian continuous permafrost region, snow persists throughout winter, with the snow cover fraction typically close to 100%. As a result, the interannual variability of winter snow cover fraction is small (Figure S2a–c), and its influence on T_{soil} can be considered negligible in winter. In contrast, d_{snow} exhibits substantial interannual variability in winter over central and western Siberia (Figure S2d–f). Regions characterized by large d_{snow} variability generally coincide with those showing a pronounced increase in the interannual variability of T_{soil}, suggesting that d_{snow} fluctuations may help explain the changes in T_{soil} variability. Given that previous studies have established a relation between d_{snow} and T_{soil} (*Zhang,* 2005; *Park et al.,* 2015; *Wang et al.,* 2016; *Zhang et al.,* 2018; *Zhong et al.,* 2025), this study focuses on whether their interannual variabilities are similarly linked.

https://doi.org/10.5194/egusphere-2025-5676
Preprint. Discussion started: 19 February 2026

Based on Globsnow dataset and in-situ observations, both winter d_{snow} and its interannual variability exhibit a significant increasing trend since 1990s (Figure 4a), generally synchronized with the increase in winter T_{soil} interannual variability. Spatially, after 1990s, the interannual variability of winter d_{snow} significantly increased across most of the Siberian continuous permafrost region (Figure 4b), strong increases in variability are concentrated in central and western Siberia, particularly in the western region where snow is generally thick (Figure S2). Although sporadic regions of weak and localized decreases are observed, their extent and magnitude are minor compared with the widespread increases. In addition, the average snow depth in Siberia before the 1990s was generally lower before the 1990s than that in later periods, which partly explains why the interannual variability of soil temperature was reduced prior to the 1990s. With thinner snow, its insulating effect on the soil was limited, and the rapid rise of winter soil temperature was primarily driven by background air temperature. The recently observed decoupling between air temperature and soil temperature in northern Eurasia provides some support for this conclusion (*Chen et al.,* 2021).

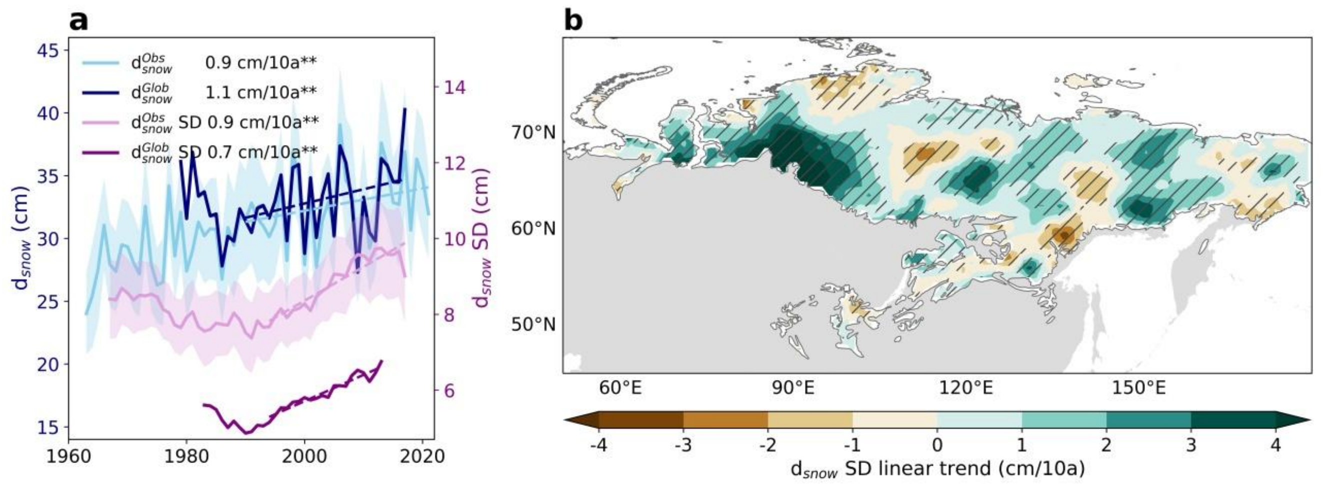

Figure 4: Spatiotemporal changes in winter snow depth (d_{snow}) interannual variability. **(a)** Long-term evolution of d_{snow} and its 9-year sliding standard deviation (SD; cm) based on the Globsnow dataset (1979–2018) and in-situ observations (1963–2022), Dashed line indicate trends since 1990 in d_{snow} and 1993 in d_{snow} SD, with significance denoted by '**'. **(b)** Spatial distribution of linear trends in interannual SD of d_{snow} (cm/10a) since 1993, with black hatching indicating significant areas. All significance was assessed using Student's t-test ($p < 0.05$).

The increase in winter d_{snow} variability implies more frequent extreme snowfall events. Probability density analysis further shows that interannual extreme changes in d_{snow} have intensified after 1990s (Figure 5a). Specifically, positive extremes (extreme thickening) shifted markedly compared with the pre-1993 period, becoming mainly concentrated within 2–3 standard deviations. Negative extremes (extreme thinning) also increased within the 2–3 standard deviation range, but their probability and intensity were smaller than the positive extremes. It's confirmed that d_{snow} interannual variability has become larger, dominated by extreme increases. Notably, interannual extremes in T_{soil} exhibit a consistent pattern of enhancement in parallel with d_{snow}, predominantly reflecting extreme warming (Figure 5b). These results point to a potential intrinsic link between the increased STRI and lager d_{snow} fluctuations since 1990s.

https://doi.org/10.5194/egusphere-2025-5676
Preprint. Discussion started: 19 February 2026

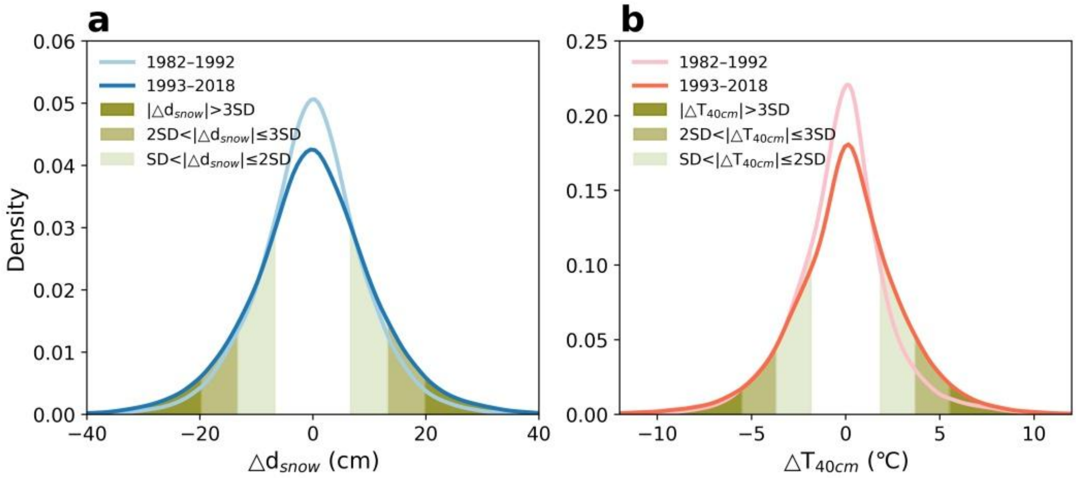

Figure 5: Probability density distributions of interannual changes in d_{snow} (Δd_{snow}; cm) and T_{soil} (ΔT_{soil} ;°C) before and after 1993. **(a)** d_{snow} from Globsnow; **(b)** T_{soil} from merged data. Shaded areas indicate ±1, ±2, and ±3 standard deviations calculated for 1982–2018.

To further quantify relationship between d_{snow} interannual variability and STRI, we firstly accounted for the potential influence of air temperature (T_{air}), which has been shown to strongly affect T_{soil} (*Amato et al.,* 2024; *Zhong et al.,* 2025). A multiple linear regression approach was applied to quantify and remove the effects of autumn and winter T_{air} on winter T_{soil} variability, followed by normalization. The results indicate that, in the Siberian continuous permafrost region, the impact of winter T_{air} on winter STRI is limited, whereas autumn T_{air} exerts a moderate influence in central and western Siberia, generally contributing less than 50% (Figure S3). This pattern likely arises because higher autumn T_{air}, occurring before the soil surface is completely frozen, promote downward heat conduction and establish warmer initial soil conditions for winter. In winter, as T_{soil} is generally higher than near-surface T_{air} (Figure S4c), the ground-air heat flux reverses upward. Meanwhile, d_{snow} becomes substantially thicker than in autumn, further impeding heat exchange between the soil and the near-surface atmosphere and weakening the coupling between them.

After excluding the T_{air} effect, correlation analyses between STRI and d_{snow} variability in winter were conducted. The results reveal a positive correlation between d_{snow} SD and T_{soil} SD at both 40 cm and 160 cm depths across most parts of the study region (Figure 6), with strong consistency between in-situ observations and the gridded datasets. Significant positive correlations are mainly distributed over central and western Siberia, spatially coinciding with regions of increased STRI (Figure 3). Moreover, the extent of significant correlation at 160 cm is slightly narrower than that at 40 cm, implying a delayed and attenuated subsurface response.

https://doi.org/10.5194/egusphere-2025-5676
Preprint. Discussion started: 19 February 2026

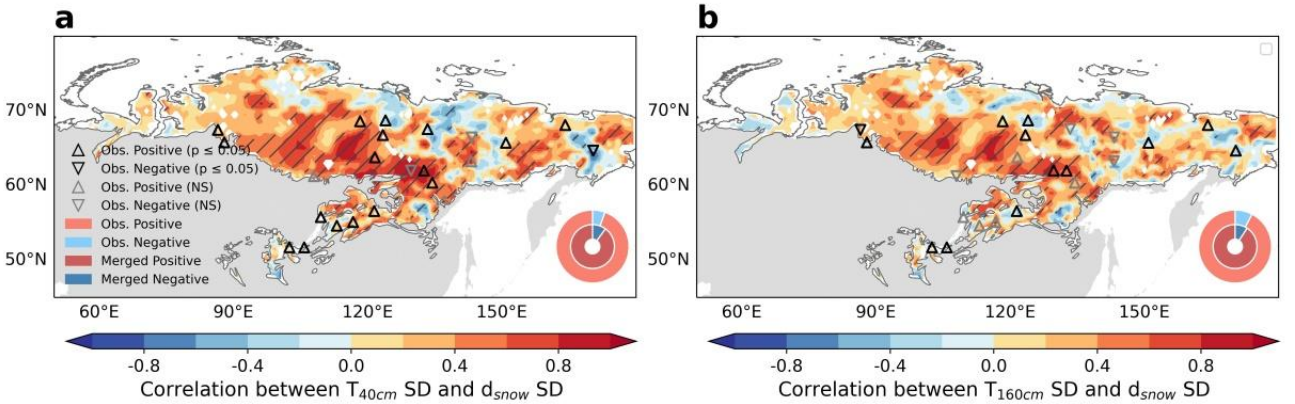

Figure 6: Relationship between interannual variabilities of winter snow depth (d_{snow}) and STRI since 1990s. Correlation analysis between T_{soil} standard deviation (SD) at 40 cm **(a)** and 160 cm **(b)** depths and d_{snow} SD. Shaded areas with black hatching indicate significant correlations between the two variables based on gridded data. Triangles represent correlations calculated based on in-situ observations, with black outlines indicating significance. Pie charts in the lower right summarize the proportion of significant positive and negative correlations. All significance was assessed using Student's t-test ($p < 0.05$).

Previous studies have indicated that variations in d_{snow} can also influence the surface albedo (*Roesch et al.,* 2001; *Barlage et al.,* 2010). However, the statistical relationship between d_{snow} and surface albedo is insignificant in most regions (Figure S4a). This may be attributed to the thick snow in Siberia and the fact that surface albedo depends more on the snow cover fraction. For shallow snow, albedo increases with d_{snow}, but once d_{snow} exceeds 10 cm, albedo stabilizes around 0.8 (*Barlage et al.,* 2010). Given that d_{snow} in Siberia typically exceeds 20 cm (Figure S2), this results in an insignificant relationship between d_{snow} and surface albedo. Instead, the primary influence of winter snow on T_{soil} manifests through its thermal insulation effect, which effectively retains heat and protects the underlying soil from extreme cold.

It should be noted that, the feedback of T_{soil} to d_{snow}, primarily through snowmelt, can be considered negligible. The percentage of snowmelt is below 10% in most regions (Figure S4b), since both air and soil temperatures generally remain below -5 °C during winter (Figure S4c,d). Consequently, the snow-soil interaction in winter should be dominated by d_{snow}. In other words, the increased STRI is closely linked to the increased interannual fluctuations in snow depth.

3.3 Dominant role of snow depth interannual fluctuations in winter STRI demonstrated by numerical experiments

To further explore the role of d_{snow} variability in increased winter STRI in Siberian continuous permafrost region through its thermal insulation effect, CTL and SE experiments (the detail seen in Section 2.5) were conducted to quantify the response of soil thermal regime to the changes in winter d_{snow} variability. In the SE experiment, the interannual fluctuations of snowfall in autumn and winter were removed to weaken the interannual variability of winter d_{snow}. Snow accumulation across the Siberian continuous permafrost region is generally thick, particularly over central-western Siberia, where the winter mean snowfall reaches 60 to 100 cm (Figure 7a), and the mean d_{snow} generally exceeds 40 cm, with a typical interannual variability of 6–10 cm (Figure S2). It has been indicated that the optimal snow depth for maintaining maximal

https://doi.org/10.5194/egusphere-2025-5676
Preprint. Discussion started: 19 February 2026

thermal insulation ranges from 40 to 70 cm (*Zhang et al.*, 2021), this suggests that snow depth in this region is already close to the optimal range for thermal insulation. The red box in Figure 7a marks a typical region in central Siberia for investigating how d_{snow} variability influences soil thermal stability, this region coincides with the zones showing large interannual variability trends in both T_{soil} (Figure 3) and d_{snow} (Figure 4), as well as a significant positive correlation between them (Figure 6). Since October, the mean T_{air} over the Siberian continuous permafrost region has dropped below -10 °C (Figure S4c), indicating that precipitation during autumn and winter primarily falls as snow. The regional mean instantaneous precipitation rate time series from the CTL and SE experiments show that in the CTL experiment, precipitation exhibits pronounced interannual fluctuations during autumn and winter, whereas in the SE experiment, interannual variability of snowfall in autumn and winter was removed, the time series becomes much smoother (Figure 7b–g). These results confirm that the SE experiment effectively suppressed the interannual fluctuations of snowfall, successfully achieving the intended forcing condition.

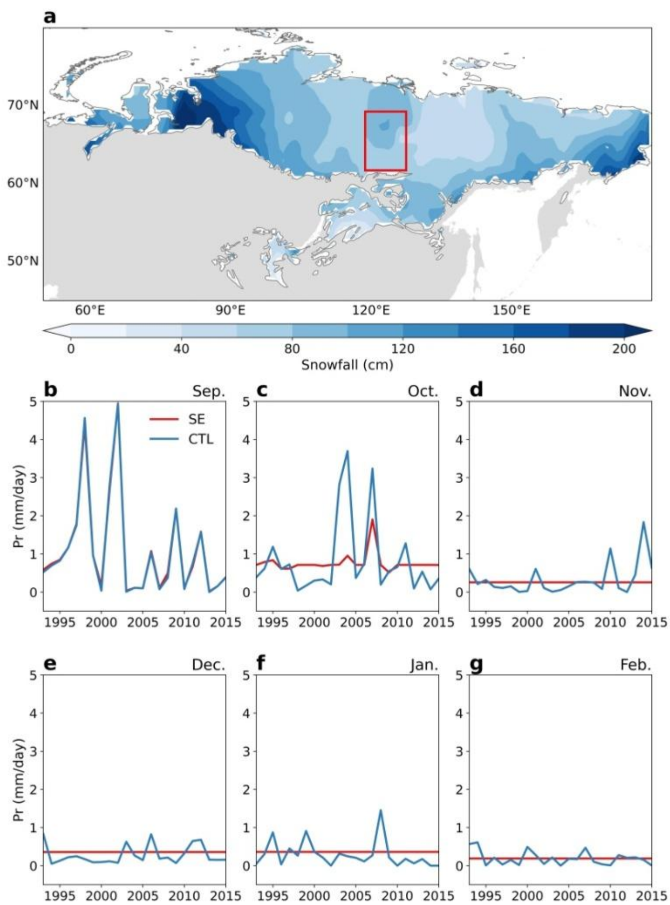

Figure 7: Evolution of snowfall from CTL and SE experiments during 1993–2015. **(a)** Spatial distribution of winter mean snowfall (cm) from the CLM simulations. The red rectangle denotes the representative region selected for time series analysis. **(b-g)** Time-series of

https://doi.org/10.5194/egusphere-2025-5676
Preprint. Discussion started: 19 February 2026

instantaneous precipitation rate (Pr; mm/day) from the CTL and SE experiments September to February, averaged over the representative region, with values taken at 03:00 UTC on the 15th day of each month.

Corresponding to the suppressed interannual variability of snowfall, interannual variability of winter d_{snow} markedly decreases (Figure 8a), the interannual variability of surface and soil heat fluxes in winter also declines accordingly (Figure 8b,c), leading to a pronounced reduction in T_{soil} variability (i.e., lower STRI) at depths of 40 cm, 160 cm, and even 358 cm (Figure 8d–f). Spatially, regions with large decreases in d_{snow} variability coincide closely with those showing strong reductions in heat flux variability and T_{soil} variability at different depths, primarily located in the central and western Siberian permafrost zone.

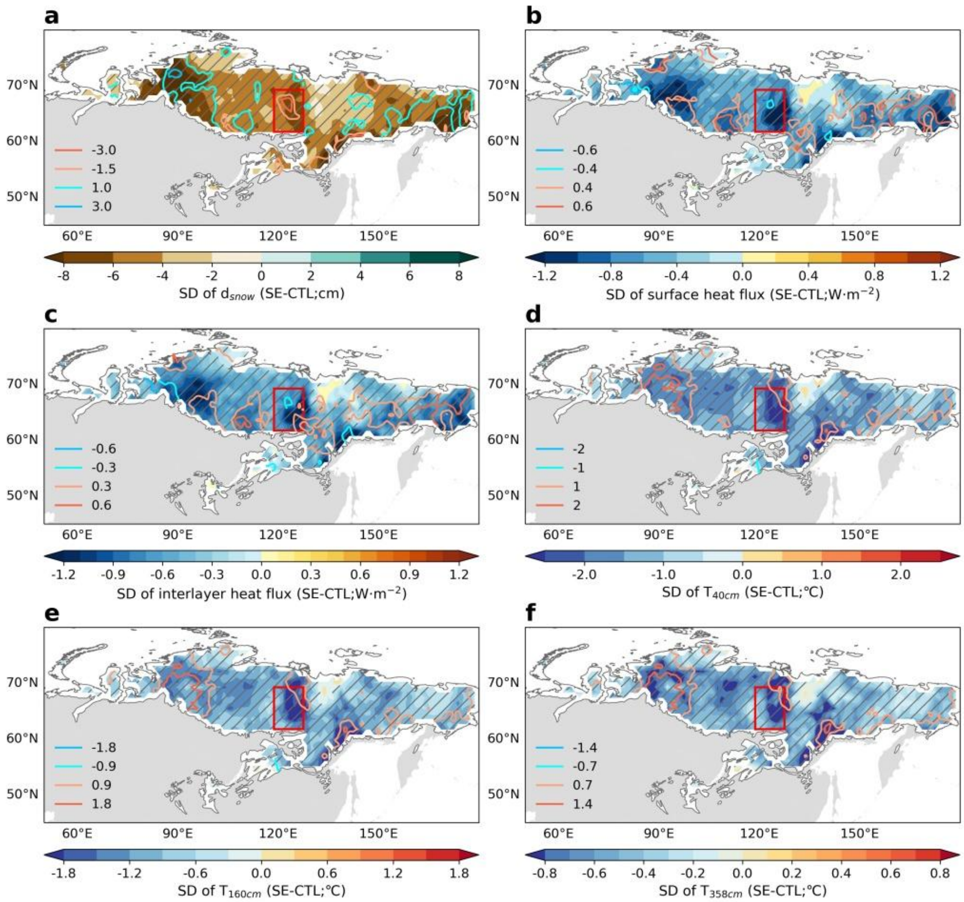

Figure 8: Simulated anomalous snow depth, soil heat flux and STRI during 1993-2011. Anomalies (SE minus CTL) of SD for **(a)** snow depth (d_{snow}; cm), **(b)** surface heat flux (W/m^2), **(c)** soil heat flux between the first and second soil layers (W/m^2), and soil temperature at depths of **(d)** 40cm (T_{40cm}), **(e)** 160cm (T_{160cm}) and **(f)** 358cm (T_{358cm}). Note that the model output at 170 cm was used as a proxy for 160 cm depth. The contours represent the anomalies values of each variable and the red rectangle denotes the representative region. The areas with gray hatching represent values significant at p<0.05 level by Student's t test.

In addition, the increasing trend of T_{soil} variability is substantially weakened, particularly in the central and western Siberian permafrost regions (Figure 9a,b). Coinciding with analysis in Sect. 3.1 and 3.2, these regions are also the centers

https://doi.org/10.5194/egusphere-2025-5676
Preprint. Discussion started: 19 February 2026

where both T_{soil} and d_{snow} variabilities have intensified rapidly since the 1990s (Figures 3 and 4), and the snow in these regions is generally thick, with an average depth exceeding ~30 cm (Figure S2). Thick snow provides strong thermal insulation that helps stabilize T_{soil} but is also more prone to large interannual fluctuations. Consequently, soils that would otherwise remain thermally stable under thick snow become increasingly unstable when d_{snow} variability intensifies.

Further time series analysis of a representative region over central Siberia shows that, compared with the CTL experiment, when the interannual variability of winter d_{snow} is substantially reduced (SE experiment), the previously significant increasing trend in T_{soil} variability at 40 cm and 160 cm depths completely disappears (Figure 9c), highlighting the crucial role of larger d_{snow} variability in increasing STRI. Moreover, although the influence of snow weakens with increasing depth, the anomalies in T_{soil} variability and their trends still propagate downward, with evident effects extending to at least 358 cm (Figure 9d,e).

Overall, the numerical experiment results demonstrate that across most of the Siberian continuous permafrost region, d_{snow} variability plays a crucial role in regulating STRI on the interannual scale. A thicker snowpack not only provides stronger thermal insulation but also exhibits larger interannual fluctuations, making soil thermal conditions particularly sensitive to snow variability, which even allows this influence to penetrate to considerable depths.

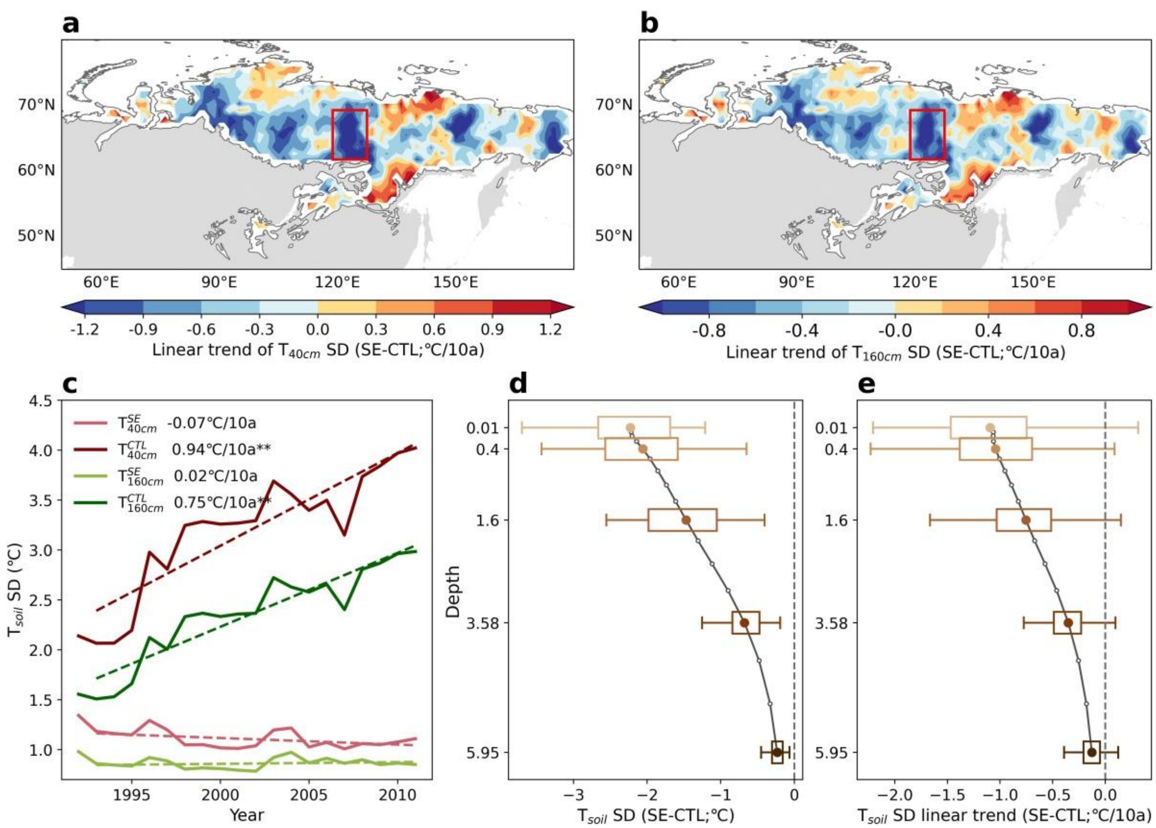

https://doi.org/10.5194/egusphere-2025-5676
Preprint. Discussion started: 19 February 2026

Figure 9: Simulated effects of decreased winter snow depth (d_{snow}) variability on STRI on the interannual scale. Spatial distribution of anomalies (SE minus CTL) in the linear trends of T_{soil} standard deviation (SD; °C/10a) at 40 cm **(a)** and 160 cm **(b)**. Note that the model output at 170 cm was used as a proxy for 160 cm depth. The red rectangle indicates the selected representative region used for analyses in c-e. **(c)** Time series of T_{soil} SD at different depths in the representative region before and after the experimental treatment, with significance by Student's t-test ($p < 0.05$) denoted by "**". Box plots showing anomalies of T_{soil} variability **(d)** and their trend **(e)** anomalies with increasing depth in the selected region. The central points indicate mean values.

Based on the numerical experiments, the contribution of d_{snow} variability to T_{soil} variability in winter over Siberian continuous permafrost regions was further quantified (Figure 10). A contribution exceeding 50% is considered to indicate a dominant role of d_{snow} variability. The results show that in central and western Siberia, d_{snow} contributes generally more than 50%. Since these regions are characterized by relatively thick snowpack, this further confirms that interannual d_{snow} variability exerts a stronger influence on T_{soil} variability, thereby enhancing STRI in areas with thicker snow.

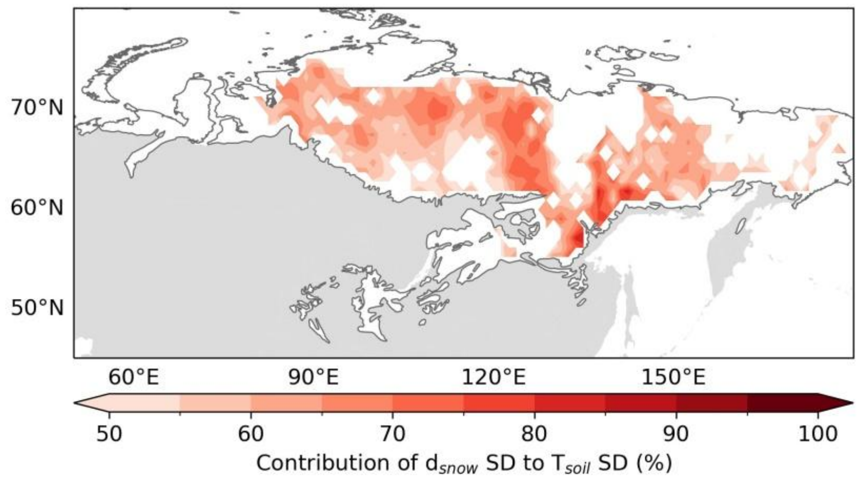

Figure 10: Spatial distribution of the contribution (%) of snow depth (d_{snow}) variability to STRI (T_{soil} variability) in winter on the interannual scale. Colored areas mark grid cells where d_{snow} explains ≥50% of T_{soil} variability; blank areas indicate a contribution <50%.

The physical process behind the effects of winter d_{snow} variability on STRI was summarized (Figure 11). Under the climatological mean state, winter T_{soil} is lower than air temperature, driving upward heat transfer from the deep soil, through the shallow soil and snow layer, and eventually into the atmosphere (Figure 11a). Essentially, d_{snow}, together with its effect on the soil–snow thermal conductivity (λ), regulates the surface heat flux and provides thermal insulation. In thick snow regions, the stronger resistance to heat transfer reduces the variability of both the soil-layer flux (F_{soil}) and the snow-to-air flux (F_1), leading to relatively stable T_{soil}, with the snowpack acting as a "buffer layer" that mitigates the impacts of atmospheric fluctuations. In contrast, shallow snow provides weaker thermal resistance, leading to relatively large T_{soil} variability. Noteworthily, after early 1990s, larger d_{snow} variability which implies more frequent anomalously heavier-snow or lighter-snow events in thick snow regions, causes larger soil heat flux variability, thereby increasing STRI (Figure 11b); whereas in thin snow regions with limited d_{snow} variability, T_{soil} is less affected.

https://doi.org/10.5194/egusphere-2025-5676
Preprint. Discussion started: 19 February 2026

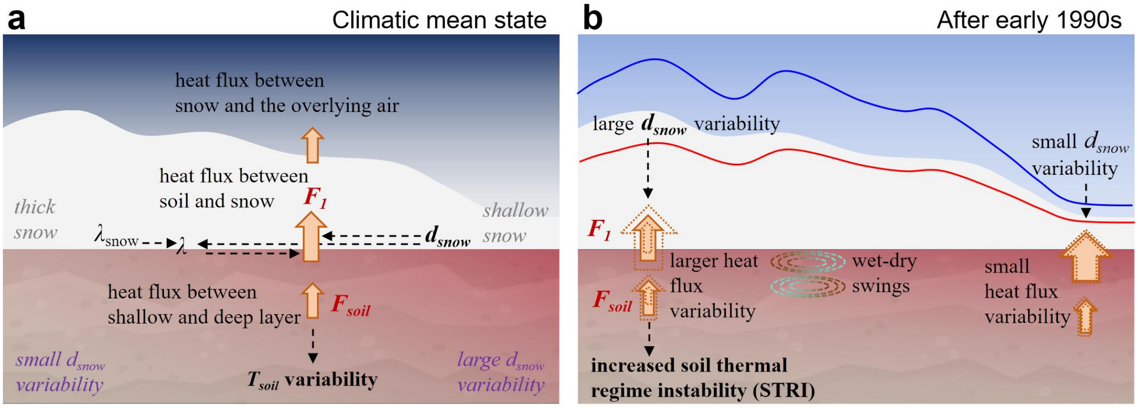

Figure 11: Schematic of physical process behind the linkage between snow depth variability and STRI. **(a)** Winter soil-snow-atmosphere heat flux pathways under the climatic mean state. **(b)** Impacts of larger interannual variability of d_{snow} on STRI after early 1990s.

4 Discussions

4.1 Potential influences of upper STRI on permafrost thermal regime

Soil thermal regimes in shallow and deep soil layers should be linked through the vertical heat transport. Across the Siberian continuous permafrost region, winter soil temperature variabilities at 40 cm and 160 cm depths exhibit significantly positive correlations (Figure 12a), which indicates that fluctuations in near-surface soil temperature can be effectively transmitted downward. Along with the increase of STRI, the depth of the freeze–thaw interface within the active layer also fluctuates on an interannual timescale. Repeated disturbances of the freeze–thaw interface modulate latent heat release and absorption, drive water and ice redistribution, promote ice lens formation, and reorganize soil pore structure, thereby altering thermal conductivity and moisture regimes (*Li et al.,* 2021*; Shi et al.,* 2024*; Zhou et al.,* 2024). As the upper boundary condition of the permafrost, these upper-layer perturbations not only directly affect deep soil temperature but also modify the efficiency of vertical heat transfer, either enhancing or delaying heat accumulation at depth, which progressively disturbing the deep thermal equilibrium and accelerating permafrost destabilization (*Zhang et al.,* 2008*; Smith et al.,* 2022*, Ran et al.,* 2022). Over Siberia permafrost region, the active layer typically does not exceed ~2.4 m in thickness (*Peng et al.,* 2018; *Li et al.,* 2022), while numerical experiments show effects of d_{snow} variability on T_{soil} can extend to at least 3.58 m (Figure 9d,e), which further supports that upper-layer temperature perturbations can penetrate through the active layer and potentially exert long-term impacts on the permafrost thermal regime. It should be noted that, the response of deeper soil to upper-layer thermal perturbations is not immediate. The lagged correlation results indicate that d_{snow} variability can influence T_{soil} variability several years later, and the soil at 160 cm depth responds to snow changes more slowly than that at 40 cm (Figure 12b). This temporal lag suggests that the thermal perturbations in upper soil induced by snow forcing act on deeper permafrost in a gradual and cumulative manner. Previous observational and modeling studies have similarly shown that the propagation of surface temperature disturbances into permafrost can take several to tens of years (*Zhang et al.,* 2008;

https://doi.org/10.5194/egusphere-2025-5676
Preprint. Discussion started: 19 February 2026

Nicolsky et al., 2018; *Smith et al.,* 2022). Therefore, this lagged relationship reveals a "thermal memory effect" in the soil system, whereby interannual fluctuations in upper-layer temperature and snow insulation can gradually weaken the thermal stability of deep permafrost over multi-year timescales.

Overall, the results suggest that larger d_{snow} variability regulates upper STRI, which in turn affects the long-term thermal stability of permafrost in a delayed and persistent manner. This highlights the necessity of incorporating both vertical heat conduction processes and temporal lag effects into permafrost modeling and projection.

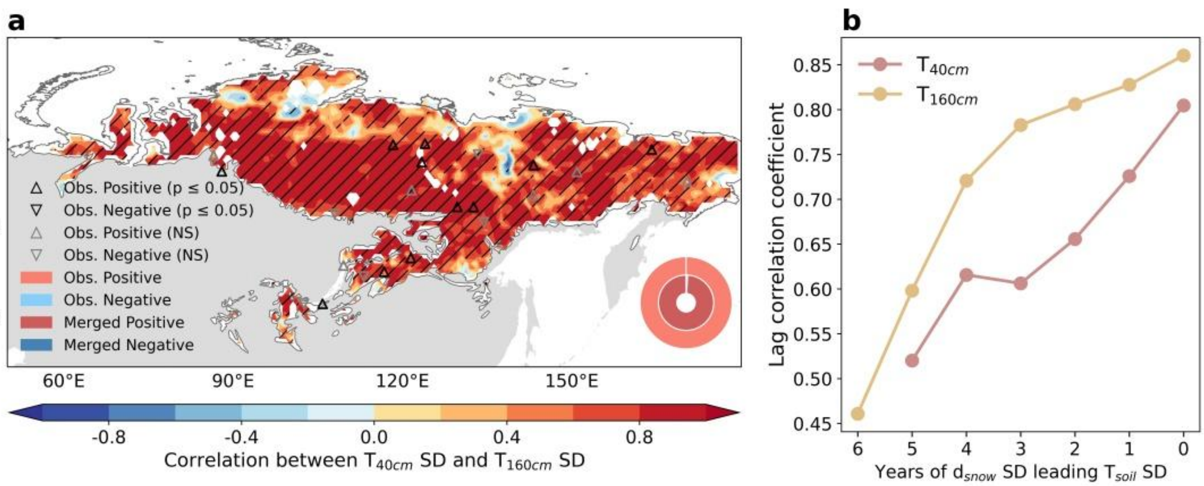

Figure 12: Spatial and temporal linkages between snow depth (d_{snow}) variability and soil thermal regime over Siberian permafrost regions since the 1990s. **(a)** Spatial correlation between interannual variability of soil temperature at 40 cm (T_{40cm} SD) and 160 cm (T_{160cm} SD) depths. Shaded areas with black hatching indicate significant correlations between the two variables based on gridded data. Triangles represent correlations calculated based on in-situ observations, with black outlines indicating significance. Pie charts in the lower right summarize the proportion of significant positive and negative correlations. **(b)** Lag correlation coefficients showing how winter d_{snow} variability leads soil temperature variability since the 1990s, based on in-situ station data. The T_{40cm} SD and T_{160cm} SD were fixed for 1993–2018, while d_{snow} SD was temporally shifted to lead the soil temperature variability, and only statistically significant results are shown. All significance was assessed using Student's t-test ($p < 0.05$).

4.2 Effects of soil water phase change on soil thermal regime

Except for near-surface air temperature and d_{snow} which influence soil-air heat exchange, soil water phase change plays a pronounced buffering role in soil heat transfer during the freeze-thaw process (*Yang and Wang*, 2019). During freezing, the release of latent heat slows down the rate of soil temperature decrease, thereby enhancing soil thermal stability to some extent (*Li et al.,* 2021). Based on the CTL experiment, the freezing of soil water at 40 cm depth mainly occurs during autumn, while changes in liquid water content in winter are almost negligible (Figure 13). Meanwhile, the liquid water content at 160 cm depth remains nearly zero from August to May of the next year, implying soil is frozen throughout the period. This indicates that the phase-change process is primarily concentrated in the shallow soil layer during autumn. In autumn when the freeze-thaw process is most active, the latent heat released during the freezing phase partially offsets the cooling induced by external temperature drops, benefiting a smooth soil temperature transition and relatively small variability in autumn

https://doi.org/10.5194/egusphere-2025-5676
Preprint. Discussion started: 19 February 2026

(Figure 1a). Once winter begins, soil is completely frozen and becomes stable, and the phase-change effect should be weakened significantly, while fluctuation in d_{snow} gradually becomes a dominant factor. Meanwhile, the increase in soil ice content enhances thermal conductivity, facilitating vertical heat transfer and further amplifying the soil temperature's response to snow variability. Consequently, the variability of winter soil temperature increases substantially. Above results suggest that soil water phase change primarily modulates the seasonal evolution of soil temperature by regulating the heat balance during the transition period.

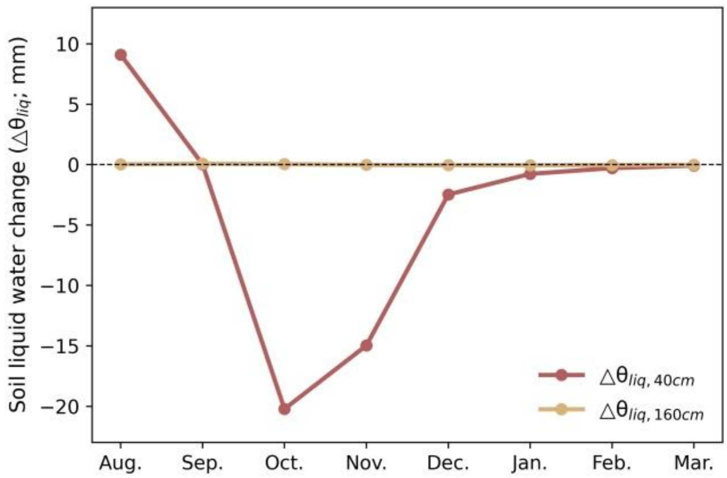

Figure 13: Monthly change in soil liquid water (Δθ; mm) at 40 cm and 160 cm depths. The values, derived from the CTL experiment, represent month-to-month differences (current month minus previous month) averaged over 1993–2016 in the Siberian continuous permafrost region.

4.3 Implication

The increased STRI indicates that surface soils overlying permafrost are experiencing more frequent and intense warm or cold anomalies. These anomalies propagate downward and accumulate, gradually affecting permafrost temperatures, reducing thermal stability, and leading to the decomposition of soil organic carbon as well as the release of carbon dioxide and methane (*Schaefer et al.,* 2014; *Pascual et al.,* 2022). In addition, the substantial ice content in surface soils means that extreme warming events could lead to rapid melting, causing ground subsidence and posing risks to infrastructure (*Yanagiya et al.,* 2020). Frequent cycles of warm-cold anomalies may also alter the vertical distribution of soil moisture in the surface layer and, through freeze-thaw processes, affect the local hydrothermal regime (*Lee et al.,* 2014; *Luo et al.,* 2024), with further impacts on local and surrounding climate (*Yang et al.,* 2019; *García-García et al.,* 2023). This study highlights that, under conditions of larger interannual variability of d_{snow}, the thermal state of soils overlying permafrost becomes more unstable, and through delayed and cumulative effects, it can affect the long-term thermal stability of permafrost, potentially leading to more carbon emissions, greater geohazard risks, and stronger permafrost feedbacks to climate system. Thus, STRI

https://doi.org/10.5194/egusphere-2025-5676
Preprint. Discussion started: 19 February 2026

not only reflects the sensitivity of the active layer to external disturbances, but can also serve as an important indicator for assessing permafrost vulnerability and potential carbon release risks.

4.4 Limitations

Although this study highlights the key role of d_{snow} in regulating soil thermal instability, several uncertainties still remain. First, in-situ observations are relatively sparse, particularly in the western regions, necessitating more long-term measurements for verification. Second, the study does not fully account for the spatial heterogeneity of surface characteristics, such as topography, vegetation, and soil type. Such heterogeneity can lead to significant local variations in STRI, including differences in d_{snow}, soil thermal conductivity, and freeze/thaw depth, which may influence assessments of active layer thickness and the thermal stability of the upper permafrost. Third, the coarse spatial resolution of the datasets and models used may fail to capture fine-scale topographic variations, micro-scale snow distribution, or vegetation differences, potentially introducing biases in simulating local STRI variability and thermal disturbances. Future research should integrate multi-source high-resolution datasets and model experiments to examine the combined effects of snow, surface characteristics, and soil properties on STRI in permafrost regions, in order to more accurately characterize thermal disturbance patterns at regional scales.

5 Conclusions

In this study, spatiotemporal variation of STRI over boreal high latitudes was investigated, and the Siberian continuous permafrost region was detected with the highest STRI in winter. Over the past 60 years, soil has exhibited a persistent warming trend, while the STRI shows declining over the long term, nevertheless, STRI markedly increases after early 1990s, suggesting a distinct shift toward the unstable soil thermal regime. This shift is particularly evident in the previously thermally stable regions of central and western Siberia, where the rate of increase in STRI exceeds 0.5 °C per decade. The rapid increased STRI indicates enhanced interannual thermal perturbations and increasing instability of the soil thermal state within the active layer in recent decades, implying increased vulnerability of the active layer and upper permafrost.

Excluding impacts of near-surface temperature, the increase in STRI is largely driven by the greater interannual variability of winter d_{snow}. The rise in d_{snow} variability corresponds closely with the increase in soil temperature variability, with both exhibiting more frequent extremes, particularly extreme soil warming and unusually thick snow events. Numerical experiments further show that reducing interannual variability in winter d_{snow} can substantially mitigate STRI, especially in central and western Siberia, with effects extending down to about 3.6 m. Quantitative analysis based on numerical experiments indicates that d_{snow} variability accounts for more than 50% of STRI in these regions.

This study also highlights the thermal disturbances in the shallow soil layer may gradually propagate downward through heat conduction, exerting a delayed cumulative influence on deep permafrost. Soil water phase change plays a buffering role during the early autumn freezing period, whereas winter d_{snow} plays a dominant role, with its fluctuations amplifying the soil thermal response by modulating soil-air heat exchange.

Code availability. The codes used for data processing and analysis are available from the corresponding author upon reasonable request.

Data availability. Permafrost zones are available from the Circum-Arctic map of permafrost and ground-ice conditions (*Brown et al.,* 2002; https://doi.org/10.7265/skbg-kf16). In-situ soil temperature and snow depth observations can be accessed through the All-Russia Research Institute for Hydro-Meteorological Information–World Data Center (http://meteo.ru/; *Sherstiukov et al.,* 2012; *Bulygina et al.,* 2012) and the UCAR/NCAR Earth Observing Laboratory (https://doi.org/10.5065/D6CN7228; *Romanovsky et al.,* 2009). ERA5-Land data are available at https://doi.org/10.24381/cds.68d2bb30 (*Muñoz-Sabater,* 2019), and ERA5 data at https://doi.org/10.5065/P8GT-0R61 (*European Centre for Medium-Range Weather Forecasts,* 2019). GLDAS-Noah datasets (versions 2.0 and 2.1) can be obtained from the Goddard Earth Sciences Data and Information Services Center (*Rodell et al.,* 2004; *Beaudoing et al.,* 2019a, 2019b; https://doi.org/10.5067/QN80TO7ZHFJZ; https://doi.org/10.5067/SXAVCZFAQLNO), along with FLDAS (*McNally and NASA/GSFC/HSL,* 2018; https://doi.org/10.5067/5NHC22T9375G) and MERRA2 (*Global Modeling and Assimilation Office,* 2015; https://doi.org/10.5067/RKPHT8KC1Y1T). CFSR (*Saha et al.,* 2010; https://doi.org/10.5065/D6DN438J) and CFSv2 (*Saha et al.,* 2012; https://doi.org/10.5065/D69021ZF) datasets are available from the NCAR Research Data Archive. GlobSnow v3.0 snow water equivalent data are accessible at https://www.globsnow.info/swe/archive_v3.0/ (*Luojus et al.,* 2021).

Author contributions. LA and KY conceived the study, with contributions from FZ, CW, and TW. LA carried out the data processing and analysis, and performed the sensitivity experiments with assistance from KY, QQ, and HL. LA wrote the manuscript. KY supervised the study and revised the manuscript. All authors contributed to the discussion and final approval of the manuscript.

Competing interests. The contact author has declared that none of the authors has any competing interests.

Acknowledgements. We acknowledge ECMWF for the ERA5 and ERA5-Land datasets, GES DISC for the GLDAS-Noah, FLDAS, and MERRA-2 datasets, and the NCAR Research Data Archive for the CFSR and CFSv2 datasets. We thank RIHMI-WDC, UCAR/NCAR EOL, and NSIDC/GlobSnow for providing the in-situ and remote-sensing observations used in this study. We also acknowledge the Circum-Arctic permafrost map as a reference dataset. We appreciate the helpful discussions and assistance from colleagues.

Financial support. This work was supported by National Key R&D Program of China (2025YFE0219100), National Natural Science Foundation of China (42305017, 42175064), National Key R&D Program of China (2020YFA0608501), Key Talent Project of Gansu Province (838104), Opening Fund of Key Laboratory of Land Surface Process and Climate Change in Cold and Arid Regions, Chinese Academy of Sciences (LPCC2023009).

https://doi.org/10.5194/egusphere-2025-5676
Preprint. Discussion started: 19 February 2026

References

Aalto, J., Scherrer, D., Lenoir, J., Guisan, A., & Luoto, M.: Biogeophysical controls on soil-atmosphere thermal differences: Implications on warming Arctic ecosystems. Environmental Research Letters, 13, 074003. https://doi.org/10.1088/1748-9326/aac83e, 2018.

Amato, M. T., & Giménez, D.: Predicting monthly near-surface soil temperature from air temperature and the leaf area index. Agricultural and Forest Meteorology, 345, 109838. https://doi.org/10.1016/j.agrformet.2023.109838, 2024.

Barlage, M., Chen, F., Tewari, M., et al.: Noah land surface model modifications to improve snowpack prediction in the Colorado Rocky Mountains. Journal of Geophysical Research: Atmospheres, 115, D22101. https://doi.org/10.1029/2009JD013470, 2010.

Beaudoing, H. and M. Rodell, NASA/GSFC/HSL.: GLDAS Noah Land Surface Model L4 monthly 0.25 x 0.25 degree V2.0 [Dataset]. Greenbelt, Maryland, USA, Goddard Earth Sciences Data and Information Services Center (GES DISC). https://doi.org/10.5067/9SQ1B3ZXP2C5, 2019a.

Beaudoing, H. & M. Rodell, NASA/GSFC/HSL.: GLDAS Noah Land Surface Model L4 monthly 0.25 x 0.25 degree V2.1 [Dataset]. Greenbelt, Maryland, USA, Goddard Earth Sciences Data and Information Services Center (GES DISC). https://doi.org/10.5067/SXAVCZFAQLNO, 2019b.

Biskaborn, B. K., et al.: Permafrost is warming at a global scale. Nature Communications, 10(1), 264. https://doi.org/10.1038/s41467-018-08240-4, 2019.

Bittelli, M., Campbell, G.S., & Tomei, F.: Soil Physics with Python: Transport in the Soil-Plant-Atmosphere System. Oxford University Press. , 2015.

Blok, D., Heijmans, M. M. P. D., Schaepman-Strub, G., Kononov, A. V., Maximov, T. C., & Berendse, F.: Shrub expansion may reduce summer permafrost thaw in Siberian tundra. Global Change Biology, 16, 1296–1305. https://doi.org/10.1111/j.1365-2486.2009.02110.x, 2010.

Brown, J., Ferrians, O. J. J., Heginbottom, J. A. & Melnikov, E. S.: CircumArctic Map of Permafrost and Ground-Ice Conditions (GGD318, Version 2) [Dataset]. National Snow and Ice Data Center. https://doi.org/10.7265/skbg-kf16, 2002.

Brutsaert, W., Cheng, L., & Zhang, L.: Spatial Distribution of Global Landscape Evaporation in the Early Twenty-First Century by Means of a Generalized Complementary Approach. https://doi.org/10.1175/JHM-D-19-0208.1, 2020.

Bulygina, O. N., & Razuvaev, V. N.: Daily Temperature and Precipitation Data for 518 Russian Meteorological Stations (1881-2010) [Dataset]. Carbon Dioxide Information Analysis Center. https://doi.org/10.3334/CDIAC/cli.100, 2012.

Chen, L., Aalto, J., & Luoto, M.: Significant shallow–depth soil warming over Russia during the past 40 years. Global and Planetary Change, 197, 103394. https://doi.org/10.1016/j.gloplacha.2020.103394, 2021.

https://doi.org/10.5194/egusphere-2025-5676
Preprint. Discussion started: 19 February 2026

Chen, P.-J., Wu, C.-H., Chen, Y.-G., & Lee, S.-Y.: Impact of Solar Activity and ENSO on the Early Summer Asian Monsoon During the Last Millennium. Geophysical Research Letters, 51(3), e2023GL105668. https://doi.org/10.1029/2023GL105668, 2024.

Davidson, E. A., & Janssens, I. A.: Temperature sensitivity of soil carbon decomposition and feedbacks to climate change. Nature, 440, 165–173. https://doi.org/10.1038/nature04514, 2006.

European Centre for Medium-Range Weather Forecasts.: ERA5 Reanalysis (Monthly Mean 0.25 Degree Latitude-Longitude Grid) [Dataset] . NSF National Center for Atmospheric Research. https://doi.org/10.5065/P8GT-0R61, 2019.

Foster, G., & Rahmstorf, S.: Global temperature evolution 1979–2010. Environmental Research Letters, 6(4), 044022. https://doi.org/10.1088/1748-9326/6/4/044022, 2011.

Fu, Z.-T., Wu, Q.-B., Wang, L.-Y., & Liu, Y.-L. Response of soil hydrothermal processes within the active layer to variable alpine vegetation conditions on the Qinghai–Tibet Plateau. Advances in Climate Change Research, 14(2), 200–212. https://doi.org/10.1016/j.accre.2023.03.003, 2023.

García-García, A., et al.: Soil heat extremes can outpace air temperature extremes. Nature Climate Change, 13, 1237–1241. https://doi.org/10.1038/s41558-023-01812-3, 2023.

Global Modeling and Assimilation Office (GMAO).: MERRA-2 tavg1_2d_lnd_Nx: 2d,1-Hourly,Time-Averaged,Single-Level,Assimilation,Land Surface Diagnostics V5.12.4 [Dataset]. Greenbelt, MD, USA, Goddard Earth Sciences Data and Information Services Center (GES DISC). https://doi.org/10.5067/RKPHT8KC1Y1T, 2015.

Gottlieb, A.R., & Mankin, J.S.: Evidence of human influence on Northern Hemisphere snow loss. Nature, 625, 293–300. https://doi.org/10.1038/s41586-023-06794-y, 2024.

Groisman, P., et al.: Northern Eurasia Future Initiative (NEFI): Facing the challenges and pathways of global change in the twenty-first century. Progress in Earth and Planetary Science, 4, 41. https://doi.org/10.1186/s40645-017-0154-5, 2017.

Hagerty, S., et al.: Accelerated microbial turnover but constant growth efficiency with warming in soil. Nature Climate Change, 4, 903–906. https://10.1038/nclimate2361, 2014.

Heijmans, M. M. P. D., et al.: Tundra vegetation change and impacts on permafrost. Nature Reviews Earth & Environment, 3, 68–84. https://doi.org/10.1016/j.accre.2020.07.002, 2022.

Jiang, Y., Zhuang, Q., Sitch, S., et al. Importance of soil thermal regime in terrestrial ecosystem carbon dynamics in the circumpolar north. Global and Planetary Change, 142, 28–40. https://doi.org/10.1016/j.gloplacha.2016.04.011, 2016.

Jordan, R.: A one-dimensional temperature model for a snow cover: Technical documentation for SNTHERM (Special Report 49). U.S. Army Corps of Engineers, 89 pp. https://erdc-library.erdc.dren.mil/server/api/core/bitstreams/81b728f8-8f72-4ef8-e053-411ac80adeb3/content, 1991.

Karl, T. R., Knight, R. W., & Plummer, N.: Trends in high-frequency climate variability in the twentieth century. Nature, 377, 217–220. https://doi.org/ 10.1038/377217a0, 1995.

https://doi.org/10.5194/egusphere-2025-5676
Preprint. Discussion started: 19 February 2026

Lawrence, D. M., et al.: The Community Land Model version 5: Description of new features, benchmarking, and impact of forcing uncertainty. Journal of Advances in Modeling Earth Systems, 11, 4245–4287. https://doi.org/10.1029/2018MS001583, 2019.

Lee, H., Swenson, S. C., Slater, A. G., & Lawrence, D. M.: Effects of excess ground ice on projections of permafrost in a warming climate. Environmental Research Letters, 9, 124006. https://doi.org/10.1088/1748-9326/9/12/124006, 2014.

Li, Q., Xue, Y., & Liu, Y.: Impact of frozen soil processes on soil thermal characteristics at seasonal to decadal scales over the Tibetan Plateau and North China. Hydrology and Earth System Sciences, 25(4), 2089–2107. https://doi.org/10.5194/hess-25-2089-2021, 2021.

Li, C., Wei, Y., Liu, Y., Li, L., Peng, L., Chen, J., Liu, L., Dou, T., & Wu, X.: Active Layer Thickness in the Northern Hemisphere: Changes From 2000 to 2018 and Future Simulations. Journal of Geophysical Research: Atmospheres, 127(12), e2022JD036785. https://doi.org/10.1029/2022JD036785, 2022.

Liu, W., Li, R., Wu, T., Hu, G., et al.: Comparative analysis of soil thermal conductivity in the permafrost regions of the Qinghai–Tibetan Plateau and the Arctic. Geoderma, 460, 117409. https://doi.org/10.1016/j.geoderma.2025.117409, 2025.

Liu, Y., Hansen, B. U., Elberling, B., & Westergaard-Nielsen, A.: Snow depth and the associated offset in ground temperatures in a landscape manipulated with snow-fences. Geoderma, 438, 116632. https://doi.org/10.1016/j.geoderma.2023.116632, 2023.

Loranty, M. M., Abbott, B. W., Blok, D., Douglas, T. A., Epstein, H. E., Forbes, B. C., Jones, B. M., Kholodov, A. L., Kropp, H., Malhotra, A., Mamet, S. D., Myers-Smith, I. H., Natali, S. M., O'Donnell, J. A., Phoenix, G. K., Rocha, A. V., Sonnentag, O., Tape, K. D., and Walker, D. A.: Reviews and syntheses: Changing ecosystem influences on soil thermal regimes in northern high-latitude permafrost regions, Biogeosciences, 15, 5287–5313, https://doi.org/10.5194/bg-15-5287-2018, 2018.

Luo, C., Wang, R., Hao, K., Jia, X., Zhu, J., Xin, Z., & Xiao, H.: Effects of Seasonal Freezing and Thawing on Soil Moisture and Salinity in the Farmland Shelterbelt System in the Hetao Irrigation District. Agronomy, 14(7), 1425. https://doi.org/10.3390/agronomy14071425, 2024.

Luojus, K., Pulliainen, J., Takala, M. et al.: GlobSnow v3.0 Northern Hemisphere snow water equivalent dataset. Sci Data, 8, 163. https://doi.org/10.1038/s41597-021-00939-2, 2021.

Mudryk, L. R., et al.: Historical Northern Hemisphere snow cover trends and projected changes, The Cryosphere, 14, 2495–2514. https://doi.org/10.5194/tc-14-2495-2020, 2020.

Muñoz Sabater, J.: ERA5-Land monthly averaged data from 1950 to present [Dataset]. Copernicus Climate Change Service (C3S) Climate Data Store (CDS). https://doi.org/10.24381/cds.68d2bb30, 2019.

McNally, A. & NASA/GSFC/HSL.: FLDAS Noah Land Surface Model L4 Global Monthly 0.1 x 0.1 degree (MERRA-2 and CHIRPS) [Dataset]. Greenbelt, MD, USA, Goddard Earth Sciences Data and Information Services Center (GES DISC). https://doi.org/10.5067/5NHC22T9375G, 2018.

Nicolsky, D. J., & Romanovsky, V. E.: Modeling Long-Term Permafrost Degradation. Journal of Geophysical Research: Earth Surface, 123(8), 1756–1771. https://doi.org/10.1029/2018JF004655, 2018.

Noetzli, J., & Gruber, S.: Transient thermal effects in Alpine permafrost. The Cryosphere. 3, 85–99. https://doi.org/10.5194/tc-3-85-2009, 2009.

Paquin, J.-P., & Sushama, L.: On the Arctic near-surface permafrost and climate sensitivities to soil and snow model formulations in climate models. Climate Dynamics, 44(1), 203–228. https://doi.org/10.1007/s00382-014-2185-6, 2015.

Park, H., Fedorov, A. N., Zheleznyak, M. N., Konstantinov, P. Y., & Walsh, J. E.: Effect of snow cover on pan-Arctic permafrost thermal regimes. Climate Dynamics, 44, 2873–2895. https://doi.org/10.1007/s00382-014-2356-5, 2015.

Paul, K. I., Polglase, P. J., Smethurst, P. J., O'Connell, A. M., Carlyle, C. J., & Khanna, P. K.: Soil temperature under forests: A simple model for predicting soil temperature under a range of forest types. Agricultural and Forest Meteorology, 121(3), 167–182. https://doi.org/10.1016/j.agrformet.2003.08.030, 2004.

Peng, X., Zhang, T., Frauenfeld, O. W., Wang, K., Luo, D., Cao, B., Su, H., Jin, H., & Wu, Q.: Spatiotemporal Changes in Active Layer Thickness under Contemporary and Projected Climate in the Northern Hemisphere. Journal of Climate, 31(1), 251–266. https://doi.org/10.1175/JCLI-D-16-0721.1, 2018.

Pepin, N., et al.: Elevation-dependent warming in mountain regions of the world. Nature Climate Change, 5, 424–430. https://doi.org/10.1038/nclimate2563, 2015.

Pugh, T. A. M., Rademacher, T., Shafer, S. L. et al.: Understanding the uncertainty in global forest carbon turnover. Biogeosciences, 17(15), 3961～3989. https://doi.org/10.5194/bg-17-3961-2020, 2020.

Pulliainen, J., Luojus, K., Derksen, C. et al.: Patterns and trends of Northern Hemisphere snow mass from 1980 to 2018. Nature, 581, 294–298. https://doi.org/10.1038/s41586-020-2258-0, 2020.

Pascual, D., & Johansson, M.: Increasing impacts of extreme winter warming events on permafrost, Weather and Climate Extremes, 36, 100450. https://doi.org/10.1016/j.wace.2022.100450, 2022.

Quante, L., Willner, S.N., Middelanis, R. et al.: Regions of intensification of extreme snowfall under future warming. Scientific Reports, 11, 16621. https://doi.org/10.1038/s41598-021-95979-4, 2021.

Ran, Y., Li, X., Cheng, G., et al.: New high-resolution estimates of the permafrost thermal state and hydrothermal conditions over the Northern Hemisphere, Earth Syst. Sci. Data, 14, 865–884, https://doi.org/10.5194/essd-14-865-2022, 2022.

Rantanen, M., et al.: The Arctic has warmed nearly four times faster than the globe since 1979. Communications Earth & Environment, 3, 168. https://doi.org/10.1038/s43247-022-00498-3, 2022.

Rodell, M., P.R. Houser, U. Jambor, et al.: The Global Land Data Assimilation System. Bulletin of the American Meteorological Society, 85, 381-394, https://doi.org/10.1175/BAMS-85-3-381, 2004.

Roesch, A., Wild, M., Gilgen, H., & Ohmura, A.: A new snow cover fraction parametrization for the ECHAM4 GCM. Climate Dynamics, 17, 933–946. https://doi.org/10.1007/s003820100153, 2001.

Romanovsky, V.: East Siberian air, ground temperature, and snow depth measurements, 1882–1994 (version 1.0) [Dataset]. UCAR/NCAR-Earth Observing Laboratory. https://doi.org/10.5065/D6CN7228 , 2009.

Romanovsky, V. E., Smith, S. L., & Christiansen, H. H.: Permafrost thermal state in the polar Northern Hemisphere during the international polar year 2007–2009: A synthesis. Permafrost and Periglacial Processes, 21, 106–116. https://doi.org/10.1002/ppp.689, 2010.

Rooney, E. C., Bailey, V. L., Patel, K. F., et al.: Soil pore network response to freeze-thaw cycles in permafrost aggregates. Geoderma, 411, 115674. https://doi.org/10.1016/j.geoderma.2021.115674, 2022.

Saha, S., et al.: NCEP Climate Forecast System Reanalysis (CFSR) Monthly Products, January 1979 to December 2010 [Dataset]. NSF National Center for Atmospheric Research. https://doi.org/10.5065/D6DN438J, 2010.

Saha, S., et al.: NCEP Climate Forecast System Version 2 (CFSv2) Monthly Products [Dataset]. NSF National Center for Atmospheric Research. https://doi.org/10.5065/D69021ZF, 2012.

Schaefer, K., Lantuit, H., Romanovsky, V. E., Schuur, E. A. G., & Witt, R.: The impact of the permafrost carbon feedback on global climate. Environmental Research Letters, 9(8), 085003. https://doi.org/10.1088/1748-9326/9/8/085003, 2014.

Schuur, E. A. G., et al.: Climate change and the permafrost carbon feedback. Nature, 520, 171–179. https://doi.org/10.1038/nature14338, 2015.

Seneviratne, S. I., et al.: Impact of soil moisture-climate feedbacks on CMIP5 projections: First results from the GLACE-CMIP5 experiment. Geophysical Research Letters, 40, 5212–5217. https://doi.org/10.1002/grl.50956, 2013.

Sherstiukov, A.: Daily data set of soil temperature at depths to 320 cm from meteorological stations of the Russian Federation [Dataset]. RIHMI-WDC. https://meteo.ru/english/climate/soil, 2012.

Shi, Y., Zhang, L., Mu, Y., Ma, W., Kong, X., & Yang, C.: Dynamic characteristics of soil pore structure and water-heat variations during freeze-thaw process. Engineering Geology, 343, 107785. https://doi.org/10.1016/j.enggeo.2024.107785, 2024.

Smith, S. L., O'Neill, H. B., Isaksen, K., Noetzli, J., & Romanovsky, V. E.: The changing thermal state of permafrost. Nature Reviews Earth & Environment, 3(1), 10–23. https://doi.org/10.1038/s43017-021-00240-1, 2022.

Soong, J. L., Phillips, C. L., Ledna, C., Koven, C. D., & Torn, M. S.: CMIP5 models predict rapid and deep soil warming over the 21st century. Journal of Geophysical Research: Biogeosciences, 125, e2019JG005266. https://doi.org/10.1029/2019JG005266, 2020.

Stieglitz, M., Déry, S. J., Romanovsky, V. E., & Osterkamp, T. E.: The role of snow cover in the warming of arctic permafrost. Geophysical Research Letters, 30, 2003GL017337. https://doi.org/10.1029/2003GL017337, 2003.

Style, R. W., Peppin, S. S. L., Cocks, A. C. F., & Wettlaufer, J. S.: Ice-lens formation and geometrical supercooling in soils and other colloidal materials. Physical Review E, 84(4), 041402. https://doi.org/10.1103/PhysRevE.84.041402, 2011.

Swenson, S. C., & Lawrence, D. M.: A new fractional snow - covered area parameterization for the Community Land Model and its effect on the surface energy balance. Journal of Geophysical Research: Atmospheres, 117(D21), 2012JD018178. https://doi.org/10.1029/2012JD018178, 2012.

Viovy, N.: CRUNCEP Version 7 - Atmospheric Forcing Data for the Community Land Model. NSF National Center for Atmospheric Research. https://doi.org/10.5065/PZ8F-F017, 2018.

Wang, S., Ren, L., Wu, T., et al.: Evaluating the Impact of Soil Enthalpy upon the Thawing Process of the Active Layer in Permafrost Regions of the Qinghai–Tibet Plateau Using CLM5.0. Remote Sensing 15 (1). https://doi.org/10.3390/rs15010249, 2022.

Wang, W., Rinke, A., Moore, J. C., et al.:: Evaluation of air–soil temperature relationships simulated by land surface models during winter across the permafrost region. The Cryosphere, 10, 1721–1737, https://doi.org/10.5194/tc-10-1721-2016, 2016.

Wang, R., Lu, J., Gentine, P., & Chen, H.: Global pattern of soil temperature exceeding air temperature and its linkages with surface energy fluxes. Environment al Research Letters, 19, 104029. https://doi.org/10.1088/1748-9326/ad7279, 2024.

Wright, C. K., de Beurs, K. M., & Henebry, G. M.: Land surface anomalies preceding the 2010 Russian heat wave and a link to the North Atlantic oscillation. Environmental Research Letters, 9, 124015. https://doi.org/10.1088/1748-9326/9/12/124015, 2014.

Wundram, D., Pape, R., & Löffler, J.: Alpine Soil Temperature Variability at Multiple Scales. Arctic, Antarctic, and Alpine Research, 42(1), 117–128. https://doi.org/10.1657/1938-4246-42.1.117, 2010.

Yanagiya, K., & Furuya, M.:Post-wildfire surface deformation near Batagay, Eastern Siberia, detected by L-band and C-band InSAR. Jounal of Geophysical Research: Earth Surface, 125, e2019JF005473. https://doi.org/10.1029/2019JF005473, 2020.

Yang, K., Wang, C., & Li, S.: Improved simulation of frozen-thawing process in land surface model (CLM4.5). Journal of Geophysical Research: Atmospheres, 123, 13, 238–258. https://doi.org/10.1029/2017JD028260, 2018.

Yang, K., & Wang, C.: Water storage effect of soil freeze-thaw process and its impacts on soil hydro-thermal regime variations. Agricultural and Forest Meteorology, 265, 280–294. https://doi.org/10.1016/j.agrformet.2018.11.011, 2019.

Yang, K., & Wang, C.: Frozen soil advances the effect of spring snow cover anomalies on subsequent precipitation over the Tibetan Plateau. Journal of Hydrometeorology, 24, 335–350. https://doi.org/10.1175/JHM-D-22-0083.1, 2023a.

Yang, K., Qi, Q., & Wang, C.: Possible impacts of vegetation cover increment on the relationship between winter snow cover anomalies over the Third Pole and summer precipitation in East Asia. npj Climate and Atmospheric Science, 6, 140. https://doi.org/10.1038/s41612-023-00467-3, 2023b.

You, Q., et al.: Warming amplification over the Arctic Pole and Third Pole: Trends, mechanisms and consequences. Earth-Science Reviews, 217, 103625. https://doi.org/10.1016/j.earscirev.2021.103625, 2021.

Yue, S., Che, T., Dai, L., Xiao, L., & Deng, J.: Characteristics of Snow Depth and Snow Phenology in the High Latitudes and High Altitudes of the Northern Hemisphere from 1988 to 2018. Remote Sensing, 14(19), 5057. https://doi.org/10.3390/rs14195057, 2022.

Zhang, M., Yuan, X., Otkin, J. A., & Ji, P.: Climate warming outweighs vegetation greening in intensifying flash droughts over China. Environmental Research Letters, 17(5), 054041. https://doi.org/10.1088/1748-9326/ac69fb, 2022.

Zhang, T., Barry, R. G., Gilichinsky, D., Bykhovets, S. S., Sorokovikov, V. A., & Ye, J.: An amplified signal of climatic change in soil temperatures during the last century at Irkutsk, Russia. Climatic Change, 49, 41–76. https://doi.org/10.1023/A:1010790203146, 2001.

Zhang, T.: Influence of the seasonal snow cover on the ground thermal regime: An overview. Reviews of Geophysics, 43, 2004RG000157. https://doi.org/10.1029/2004RG000157, 2005.

Zhang, W., Zhou, T., Wu， P.: Anthropogenic amplification of precipitation variability over the past century. Science, 385, 427-43. https://doi.org/10.1126/science.adp0212, 2024.

Zhang, Y., Chen, W., & Riseborough, D. W.: Disequilibrium response of permafrost thaw to climate warming in Canada over 1850–2100. Geophysical Research Letters, 35(2). https://doi.org/10.1029/2007GL032117, 2008.

Zhang, Y., Sherstiukov, A. B., Qian, B., Kokelj, S. V., & Lantz, T. C.: Impacts of snow on soil temperature observed across the circumpolar north. Environmental Research Letters, 13, 044012. https://doi.org/10.1088/1748-9326/aab1e7, 2018.

Zhao, Y., Nan, Z., Ji, H., & Zhao, L.: Convective heat transfer of spring meltwater accelerates active layer phase change in Tibet permafrost areas. The Cryosphere, 16(3), 825–849. https://doi.org/10.5194/tc-16-825-2022, 2022.

Zhong, X., Liu, Y., Zheng, L., & Kang, S.: Can snow-free breaks control soil thermal dynamics in the cold season over the warming northern Eurasia? Agricultural and Forest Meteorology, 372, 110729. https://doi.org/10.1016/j.agrformet.2025.110729, 2025.

Zhou, B., Brouchkov, A. V., & Hu, J.: Numerical Study of Pore Water Pressure in Frozen Soils during Moisture Migration. Water, 16(5). https://doi.org/10.3390/w16050776, 2024.

Zhu, D., Ciais, P., Krinner, G. et al.: Controls of soil organic matter on soil thermal dynamics in the northern high latitudes. Nature Communications, 10, 3172. https://doi.org/10.1038/s41467-019-11103-1, 2019.

Zhu, X., Wu, T., Chen, J., et al.: Summer heat wave in 2022 led to rapid warming of permafrost in the central Qinghai-Tibet Plateau. npj Climate and Atmospheric Science, 7, 216. https://doi.org/10.1038/s41612-024-00765-4, 2024.